J. Environ. Nanotechnol.
Volume 2, No. 1 (2013) pp. 52-62
ISSN (Print) : 2279-0748
ISSN (Online) : 2319-5541
DOI:10.13074/jent.2013.02.121030

Biosynthesis of Elixir of Life (Gold Nanoparticles) from Plants

Pankaj Kumar Singh,[1,2*] Subir Kundu[2]

[1]Department of Ceramic Engineering, Indian Institute of Technology, (B.H.U.), Varanasi, India.
[2]School of Biochemical Engineering, Indian Institute of Technology, (B.H.U.), Varanasi, India.

Received : 09.01.2013 Revised on : 05.02.2013 Accepted: 15.03.2013

Abstract

Biosynthesis of gold nano particles (GNPs) is considered to be a novel, effective and eco-friendly method. Biosynthesis of GNPs from *Benincasa hispida*, *Justicia gendarussa* & *Ocimum basilicum*. Biosynthesis of stable and nearly spherical GNPs using the extract of *Benincasa hispida* seeds as reducing and capping agents. The particle size could be easily tuned by the reaction conditions including quantity of extract, temperature and pH. GNP shaving different sizes in the range from10-30nm could be obtained by controlling the synthesis parameters. *Justicia gendarussa* leaf extract mediated synthesis of GNPs by the reduction of gold ions. Three different phytochemical fractions were prepared from methanolic leaf extract by liquid-liquid extraction method using immiscible solvents. The size of the GNPs ranged from 20-42nm and 62-88nm with spherical, triangle, truncated triangle and hexagonal shapes. *Ocimum basilicum* (Thai Tulsi) leaf extract worked as a potential substrate for bioreduction of $HAuCl_4$ into GNPs within 10 minutes of reaction time. It was also observed that GNPs synthesized were crystalline and uniformly spherical in shape with size range 5–40 nm which were stable even after 3 months of reaction. The gold nanoparticles were characterised by UV-Visible Spectroscopy, Transmission electron microscope (TEM), X-ray diffraction (XRD), Fourier transform infra red spectroscopy (FTIR), Dynamic light scattering (DLS), X-ray photoelectron spectroscopy (XPS) and Atomic Absorption Spectroscopy (AAS).

Keywords *: Benincasa hispida; Gold nano particles (GNPs); Justicia gendarussa; Ocimum basilicum; Transmission electron microscope (TEM).*

1. INTRODUCTION

Nanotechnology is one of the most important growth areas in the 21st century. It is thus the technology of materials dealing with very small dimension materials usually in the range of 1 to100 nm (Chin Wee Shong et al. 2010). The prefix nano comes from the Greek word for dwarf and hence nano science deals with the study of atoms, molecules and nanoscale particles in a word that is measured in nanometer (= 10^9 m). Nanoscience, the science under pinning nanotechnology is a multidisciplinary subject covering atomic, molecular& solid state physics, as well as much of chemistry. Nanostructure is known to exhibit novel and improved material properties.

Bioactive nano particle describes the beneficial or adverse effect of a nano material on living matter. A material is considered bioactive if it has interaction with or effect on any cell tissue in the human body, pharmacological activity is usually taken to describe beneficial effects, i.e the effect of drug candidates. When a nutrient is in the form that the body can easily absorb and utilize, it is said to be bioactive or bioavailable. Bones, teeth, shells, nanomagnets inside some bacteria and birds are examples of inorganic materials synthesized by biological systems. Inorganic materials inside organicmatter or organisms are known as *biocomposites* (Sulabha K. Kulkarni 2009).

*Pankaj Kumar Singh. Tel.: +91
E-mail : pankajkumarsingh2011@gmail.com

Precious metals include 6 platinum group element (PGE), silver (Ag) and gold (Au). PGE includes ruthenium (Ru), osmium (Os), rhodium (Rh), iridium (Ir), palladium (Pd) and platinum (Pt). Ru & Os, Rh & Ir, Pd & Pt and Ag & Au respectively come under 8, 9, 10 & 11 group of the transition metal (Reddi & Rao 2000).

2. MATERIALS AND METHODS

A. Isolation

Isolation of Benincasa hispida :

Benincasa hispida fruits were obtained from local market. Seeds were separated, washed thoroughly with de-ionized water and sundried. 5 g of seed was boiled in 100 mL of de-ionized water and filtered to get extract. Chloroauric acid ($HAuCl_4$) was purchased from Sigma-Aldrich (Aswathy Aromal & Daizy Philip 2012).

Isolation of Justicia gendarussa :

Justicia gendarussa plant was collected from Kanjikode hills, kerala. It was authenticated by Dr. Arumagaswamy, Plant taxonomist of KonguNadu College of Arts and Science, Coimbatore, India. The fresh leaves of *Justicia gendarussa* was washed with distilled water and shade dried for a period of one month. The dried leaves were powdered coarsely and extracted with methanol in soxhlet apparatus for 24h. The methanol extract was concentrated under reduced pressure and added to equal amount of distilled water. After 24h incubation, the chlorophyll was precipitated and removed by centrifugation at 5000 rpm for 15 minutes. The supernatant was concentrated and fractionated by immiscible solvents such as diethyl ether (Et_2O), chloroform ($CHCl_3$) and ethyl acetate (EtOAc) sequentially by liquid-liquid extraction method. Each phytochemical fraction (PF) was dried at 45°C and named as diethyl ether phytochemical fraction (Et2O-PF), chloroform phytochemical fraction ($CHCl_3$-PF) and ethyl acetate phytochemical fraction (EtOAc-PF) (Manickam Chinna et al. 2012).

Isolation of Ocimum basilicum :

$HAuCl_4$ was purchased from Qualigens fine chemicals, Mumbai, India. *Ocimum basilicum* leaves were collected from Amity University Uttar Pradesh, Noida, U.P., India. To check the accuracy and repeatability of the result the experiment was repeated thrice. 10 gm fresh leaves of *Ocimum basilicum* were collected and washed thrice with distilled water to remove dust particles. Chopped leaves were added to 100 ml water at 70ºC under continuous stirring for 30 minutes. The extract was then cooled and stored at 4ºC after filtering through Whatman No. 1 for further analysis (Garima Singhal et al. 2012).

B. Synthesis

Synthesis of GNP from Benincasa hispida :

Gold colloidg1 is prepared by adding 7.5mL extract to 30mL solution of chloroauricacid ($2.5x10^{-4}$ M) at room temperature under vigorous stirring and stirring continued for 2min. The reduction was very slow and blue color appeared after one day. Similarly colloids g_2–g_5 are prepared by adding 10 mL, 12.5 mL, 15mL and 20mL of the extract to the solution of chloroauric acid, respectively. The procedure is repeated at 373 K to get colloids g_6, g_7, g_8, g_9 and g_{10}. The reduction is found to be very fast at 373K. For g_8 fast reduction occurred as indicated by red color of the solution developed within 3 min and it is stable for more than three months. The experiment is also carried out by varying the pH of chloroauric acid and keeping the amount of extract (12.5mL) constant.The colloids g_{11}, g_{12}, g_{13}, g_{14} and g_{15} were prepared by adjusting the pH of chloroauricacid to 4, 5, 6, 7 and 8, respectively.

Synthesis of GNP from Justicia gendarussa :

1mg of each PF was separately mixed with 10ml of aqueous chloroauric acid (0.5mM) to reduce Au^{3+}. The reaction mixture was kept at room temperature for 15 minutes. The maximum production of gold nanoparticles by each PF was determined by UV-visible spectroscopy.

Synthesis of GNP from Ocimum basilicum :

Bioreduction 5 ml of leaf extract was added to 45 ml of $10^{"3}$ M $HAuCl_4$ solution at 30ºC. The reaction was observed to complete in less than 10 min.

C. Analysis

Analysis of GNP synthesized from Benincasa hispida :

The UV–vis spectra of synthesized nanoparticles were recorded on a UV-2450 Shimadzu UV spectrometer. HRTEM images and electron diffraction patterns wereobtained with a Tecnai G2 30 transmission electronmicroscope.X-ray diffraction pattern of dried nanoparticle powder was obtained using XPERT- PRO diffractometer using Cuka radiation (l¼0.1542 nm). FTIR spectra of dried gold NPS were recorded with an IR Pestige-21 Shimadzu spectrometer. The nonlinear absorption of the samples was studied with a Q-switched Nd:YAG laser delivering 532 nm with 5 ns pulse duration by Z-scan technique.

Analysis of GNP synthesized from Justicia gendarussa :

The particle size and distribution were measured in gold suspension, using dynamic light scatting (DLS) equipment (Zetasizer APS, Malvern, UK). Malvern zetasizer equipped with 10mV He-Ne laser (633nm) and operated at an angle of 90°. The morphology of synthesized GNPs was identified by TEM analysis. The sample for TEM analysis prepared on carbon coated copper grid. The TEM image was obtained by JEM-1200EX instrument operated at accelerated voltage of 120 kv. The crystalline pattern of powdered GNPs was recorded by XDL 3000 powder XRD. FT-IR analysis of the dried powder of GNPs and native diethyl ether phytochemical fraction were performed on FTIR 8201shimadzu spectrophotometer. The FTIR spectroscopic spectra were recorded in the range of 450–4000cm^{-1} at a resolution of 4 cm^{-1}.

Analysis of GNP synthesized from Ocimum basilicum :

UV-VIS Spectrophotometer Analysis: Biosynthesized gold nanoparticles were periodically analysed after 5 min and 10 min of the reaction for their optical property by UV-Vis spectroscopic studies (ELICO U.V. 165) at room temperature, operated at a resolution of 1nm between 400 nm to 650 nm range.

AAS : AAS was done to observe the conversionof $HAuCl_4$ into gold nanoparticles (GBC 932 AA).

At various stages of reaction, samples were withdrawn and centrifuged. The supernatant was analysed with AAS for concentration of gold ions in the solution. Gold ions present in the $HAuCl_4$ solution are much smaller and hence would not be separated on centrifugation, Where as Au nanoparticles are in zero valent metallic form and can be easily separated by centrifugation at around 14,500–15,000 rpm.

DLS : Size distribution of bioreduced gold nanoparticles was measured using DLS (Zetasizer Nano ZS ZEN3600, Malvern, UK). The mean size of particles inside the sample is obtained with this measurement along with correlation between the number of particles of a particular size versus the size of the GNPs.

TEM *:* TEM was done to characterize size and shape of bioreduced gold nanoparticles. After sonication (Vibronics VS 80) for 15 minutes, a drop of the sample was loaded on carbon-coated copper grids and solvent was allowed to evaporate under Infrared light for 30 minutes in vaccum. Philips model CM 200 instrument was used for TEM measurements; operated at an accelerating voltage at 200 kV.

FTIR : Vibrational bonding in sample was analyzed using FTIR measurements. After complete reduction of $HAuCl_4$ by the *Ocimum basilicum* leaf extract, the solution was centrifuged at 15,000 rpm for 15 minutes to separate gold nanoparticle from proteins or other bio-organic compounds which might interfere in analyzing protein-GNPs interaction. The Au nanoparticles pellet obtained after centrifugation were re-dispersed in water and washed (centrifugation and re-dispersion) thrice with distilled water. The samples were finally dried and mixed with KBr to form pellets and analysed on a Nicolet IR 200 (Thermo electron corp.) model.

XRD : XRD measurements of film of the biologically synthesized gold nanoparticles solution, casted onto glass slides, was done on a €MMA diffractometer. The instrument was operated at a current of 20 mA and voltage of 40 kV with Cu K (α) radiation of 1.54187 nm wavelength. Scanning was done in the region of 2θ from20° to 80° at 0.02°/ min at time constant 2s.

3. RESULTS AND DISCUSSION

GNP synthesized from *Benincasa hispida* :

UV–VIS absorption and TEM studies Fig. 1 shows the absorption spectra of gold colloids (g_1–g_5) synthesized at room temperature. Color of gold colloid is attributed to surface Plasmon resonance (SPR) arising due to collective oscillation of free conduction electrons induced by an interacting electromagnetic field (F. Toderas et al.). The position of SPR band in UV–vis spectra is sensitive to particle size, shape, local refractive index and its interaction with medium. At room temperature the reduction is slow and hence the SPR band is broad (Fig. 1) which shows the formation of particles with broad size distribution. From the spectra it is clear that when the quantity of extract is increased from 7.5mL to 12.5mL, the SPR band is shifted towards the shorter wavelength region from 548nm to 544nm which shows a decrease in particle size. But when the quantity of extract is increased from 12.5mL to 20mL, the SPR band shifted to longer wavelength region (544–553nm) which shows an increase in particle size. Thus from the results it can be inferred that at room temperature, the amount of extract is an important factor in determining the size distribution of GNPs. The reduction at 373K is faster than that at room temperature. Compared to the UV–vis spectra of gold colloids at room temperature, the SPR band of heated colloids are very narrow and also the SPR band position is shifted to shorter wavelength region which shows a decrease in particle size. Thus temperature is found to play a critical role in the size dispersity of gold nanoparticles. For the colloid g_8 a sharp peak is observed at 532 nm which is the characteristics of almost spherical nano par ticles. At pH 4, 5 and 8 the SPR band is very broad which indicates the formation of polydispersed nanoparticles.

The SPR band gets sharpened at pH6 and 7 and in colloid g_{13} a sharp peak is observed at 532nm which is the characteristics of monodispersed spherical nanoparticles. The gold colloid is more stable at a pH6 and it is stable for more than 3 months.

From the TEM images fig. 2 it is evident that the morphology of gold nanoparticles is nearly spherical which is in agreement with the shape of SPR band in the UV–vis spectra. The average particle size measured for the colloids g_3 and g_8 are observed to be 24 nm and 15 nm,

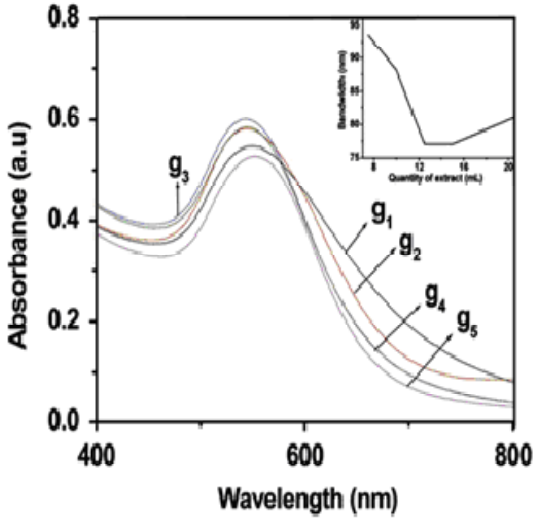

Fig. 1 : UV–vis spectra of gold colloids at room temperature (g_1) 7.5mL, (g_2) 10 mL, (g_3) 12.5mL, (g_4) 15mL and (g_5) 20mL.The inset shows the ariation of band width with quantity of extract.

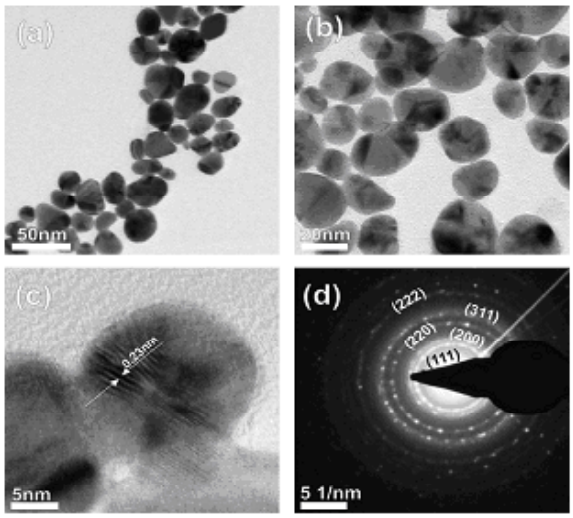

Fig. 2 : (a) and (b) TEM images of gold colloid at different magnification, (c) high resolution image and (d) SAED pattern

respectively. This shows that higher temperature during synthesis leads to a decrease in particle size. The selected area electron diffraction pattern (SAED) with brightcircular spots.

XRD analysis shows Fig. 3 the XRD pattern of dried gold nanoparticles. The XRD peaks are found to be broad indicating the formation of nanoparticles. Five diffraction peaks are observed which can be indexed to the (111), (200), (220), (311) and (222) reflections of face centered cubic structure of metallic gold, respectively, revealing that the synthesized gold nanoparticles are composed of pure crystalline gold (JCPDS no.04-0784).

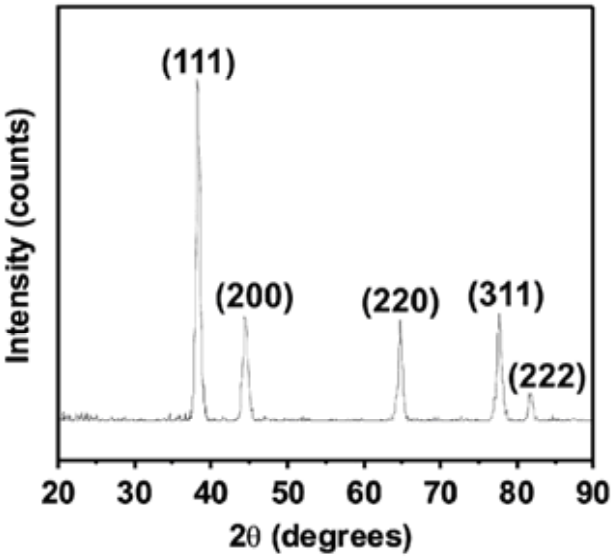

Fig. 3 : XRD pattern of gold nanoparticles

The peak corresponding to (111) plane is more intense than the other planes suggesting that (111) is the predominant orientation as confirmed by the high resolution TEM measurement. The average particle size of gold nanoparticles can be calculated using Debye–Scherrer equation.

$$D = K\lambda/b\cos\theta$$

where D is the grain size, K is the Scherrer constantwith value from 0.9 to 1, l is the wavelength of the X-ray radiation, b is the full width at half maximum and y is the Bragg angle (H. Borchert et. al.). From the Scherrer equation the average particle size of gold nanoparticles is found to be 14nm which is in agreement with the particle size measured from TEM images.

FTIR studies and mechanism of the formation of gold nanoparticles FTIR measurements were carried out to identify the possible biomolecules present in B. hispida seed extract which are responsible for the reduction and capping of GNPs. The typical FTIR spectrum of GNPs is shown in Fig. 4.

The spectrum shows bands at 1446, 1336, 1209,

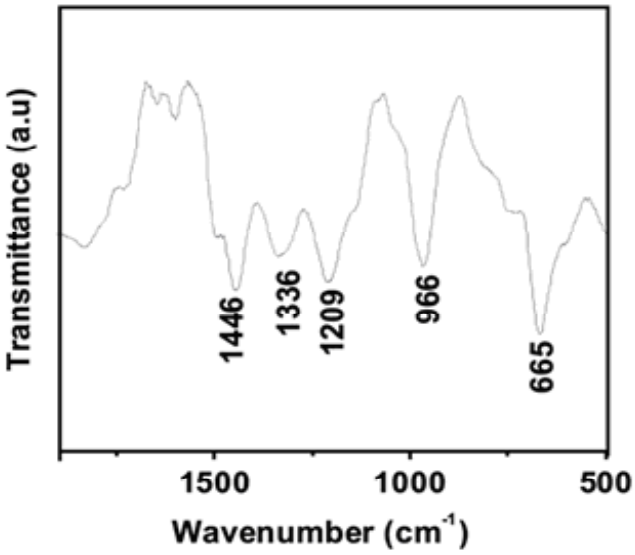

Fig. 4 : FTIR spectrum of gold nanoparticles.

966 and 665cm^{-1}. The IR absorbance corresponding to a C–O–H in-plane bend of the hydroxyl groups is observed at 1446cm^{-1} (S.L. Cumberland et al). The band at 1336 cm^{-1} is due to C–O stretching vibrations of carboxylic acid group (D. Philip). The peak located at 1209 cm^{-1} is due to stretching vibrations of C–O in polyols (D.S. Sheny et al). The absorption band at 966 cm^{-1} is assigned as C–O–C vibrations of proteins/polysaccharides present in the seed extract. The band at 665cm^{-1} might be the planebending vibration of N–H groups of proteins (S. Li et al). It is well-known that proteins can bind to GNPs through free carboxylate group (S.L. Smitha et al).

The presence of bands at 1336 cm^{-1} and 966cm^{-1} indicates that GNPs are possibly bound to proteins through carboxylate group. The phytochemical analysis of the dried seed extract of B. hispida showed the presence of carbohydrates, phenolic compounds, amino acids, proteins, flavonoids and sterols (Z.L. Qudrie et al). The polyols like poly phenols and flavonoids present in the seed extract are powerful reducing agents. The presence of band at 1209 cm^{-1} in the IR spectrum indicates that the polyols present in the seed extract may be responsible for the reduction of chloroauric acid. During the reduction process. Fig. 5) carboxylic group (COOH) present in the extract becomes COO^{-}.

This COO^{-} or the carboxylate group present in proteins can act as surfactant to attach on the surface of GNPs and it stabilizes GNPs through electrostatic stabilization. Thus it is found that B. hispida seed extract has the ability to perform dual functions of reduction and stabilization of GNPs.

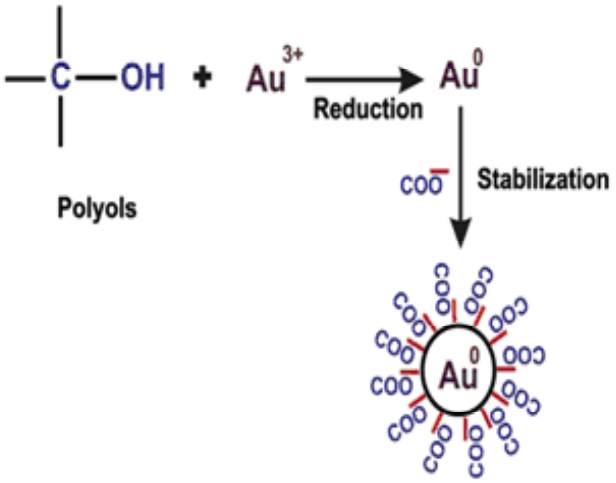

Fig. 5 : Mechanism of formation of gold nanoparticles.

GNP synthesized from *Justicia gendarussa* :

The pink-red colour developed after addition of chloroauric acid solution (10ml, 0.5 mM) into corresponding PF; each 1.0mg. Fig. 6 shows the colour of different reaction mixtures, which confirms the formation of GNPs. The colour of the reaction mixture was elicited upon excitation surface plasmon vibration with GNPs (A. Gole et al.). UV-visible spectra of each reaction mixtures were recorded after 15 minutes of incubation of chloroauric acid with corresponding PFs.

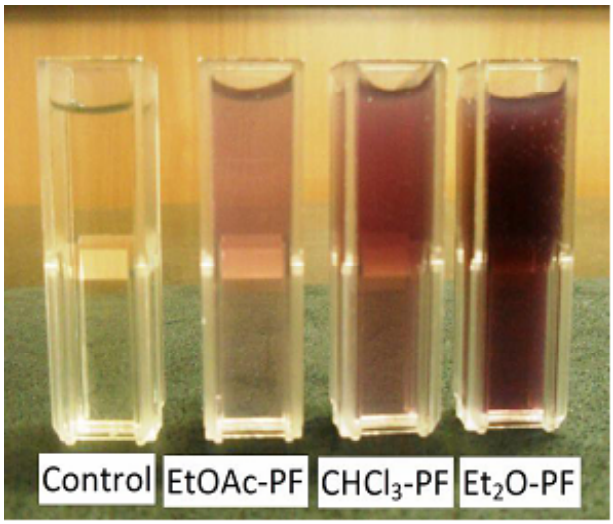

Fig. 6 : Color of synthesized GNPs after 15 minutes incubation of 0.5mm chloroauric acids with corresponding phytochemical fractions, each 1mg

Results of UV-visible spectra of gold nanoparticles synthesized by different phytochemical fraction are shown in Fig. 6**.** The maximum absorbance wavelength of gold nanoparticles was seen at 536nm. Usually absorbance value increases with increase in concentration of gold nanoparticles. Therefore measurement of absorbance at 536nm indirectly mentions about the amount of GNPs present in the reaction mixtures. The Et_2O-PF mediated synthesis of GNPs shows maximum absorbance within 15 minutes compared to $CHCl_3$-PF and EtOAc-PF mediated synthesis of GNPs. The increased production of GNPs by Et_2O-PF is due to the presence of high level of antioxidant compounds such as polyphenols and flavonoids. Polyphenols and flavonoids are important class of phytochemicals having antioxidant activity. These phytochemicals reduce metal salts like potassium ferricyanide, ferrous sulphate and chloroauric acid by donating electrons. This reducing capacity of PFs on metal ions increased with increase in concentration of polyphenols (M. Zhu). Further characterizations were done for Et_2O-PF reduced GNPs.

Each reaction mixture shows SPR band at 536 nm. The DLS results of GNPs suspension is shown in Fig. 7a, it shows two peaks. The size of GNPs are distributed in the range of 20 to 42nm (Peak1) and 62 to 88nm (peak2). The intensity of peak1 is high compared to peak2. Therefore, this concludes that most of the nanoparticles appeared in the range of 20nm to 42nm with average size of 27nm. The TEM image of GNPs is shown in Fig. 7b.

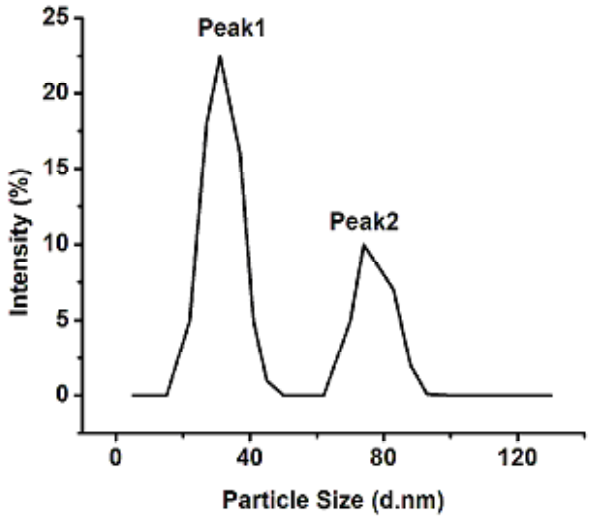

Fig. 7 a : size distribution of diethyl ether phytochemical fraction reduced gold nanoparticles measured by dls system

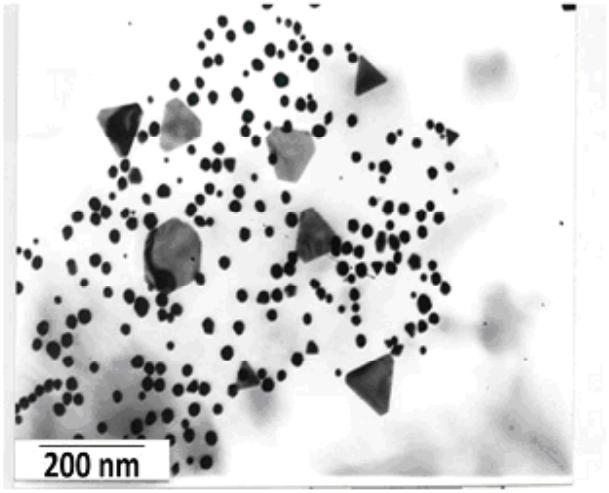

Fig. 7 b : TEM micrograph of diethyl ether phytochemical fraction reduced gold nanoparticles showing spherical, triangle, truncated triangle and hexagonal shapes

From this image, we identified that the GNPs had spherical, triangle, truncated triangle and hexagonal morphologies. Such different shaped GNPs were reported by other plant extracts such as coriander (spherical, triangle, truncated triangles and decahedral), *Coleus amboinicus* Lour (spherical, triangle, truncated triangle, hexagonal and decahedral). Synthesis of stable GNPs with various size and shape are important aspect of biomedical applications because the shape of the nanoparticles plays an important role in changing their optical properties. Z Guo *et al*. synthesized gold nano prism for biosensing application based on sensitive changes in SPR band originated by antigen-antibody recognition events. Similarly, Y-C Chuang *et al*., estimated protease activity based on optical properties of gold nano-triangles. Ankamwar *et al*., synthesized gold nano-triangles for vapor sensing applications. In recent report spherical gold nanoparticles functionalized with acetylated Dendrimers is utilized for detecting cancer cells by Computer topography imaging.

XRD analysis of powdered GNPs showed clear peaks of cubic phases (JCPDS No. 03-0921) at 38.2 (1 1 1), 44.3 (2 0 0), 64.9 (2 2 0), 77.5 (3 1 1) and 81.5 (222), which confirms the crystalline nature of GNPs. The broad bottom width of the peaks indirectly represents formation of smaller size GNPs. The FT-IR spectrum of GNPs and native Et2O–PF showed in Fig. 8. The FT-IR spectrum of GNPs and native Et_2O–PF resembles each other. Both FT-IR spectrum showed characteristic bands for alcohol (917 and 3350cm-1), C-N stretching vibration for aliphatic amines (1015 cm^{-1}), phenols (1146 cm^{-1}), C-N stretching for aromatic amines (1372cm^{-1}), germinal methyl (1442 cm^{-1}), carboxyl (1691cm^{-1}), and C-H (2849 cm^{-1}) functional groups. These bands originated from the functional groups present in the various phytochemicals of the leaf extract. From the FT-IR results, we conclude that the phytochemicals of Et_2O–PF gets adsorbed on the surface of GNPs through free amino (-NH_2) and carboxylic

(-COOH) groups makes highly stable nanoparticles.

GNP synthesized from *Ocimum basilicum* :

UV-Vis Absorbance Studies : The addition of *Ocimum basilicum* leaf extract to chloroaurate solution resulted in colour change of the solution from yellow to wine red due to the formation of gold nanoparticles. This color change arises due to the excitation of surface plasmon vibrations in case of gold nanoparticles. The surface plasmon resonance (SPR) of gold produced a peak centered near 532 nm. UV absorbance of reaction mixture taken at 5 minutes of reaction time shows peak at 537 nm indicating reduction of $HAuCl_4$ into GNPs. Sharpening of peak near 532 nm after 10 minutes of reaction time is due to blue shift in plasmon absorbance.

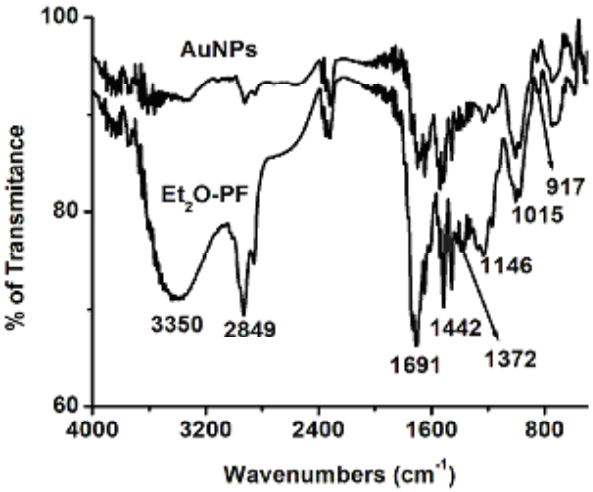

Fig. 8 : Ccomparison of FT-IR spectrum of diethyl ether phytochemical fraction and diethyl ether phytochemical fraction reduced gold nanoparticles

AAS Analysis : Gold ion concentration was analysed by AAS which showed the conversion of Au ions into GNPs. Initially standard solution of 5.5 ppm of $HAuCl_4$ was prepared and analysed with AAS at 0 min. Now, Au ion concentration in the reaction solution, after adding leaf extract, was monitored at different time intervals. Theresult showed decrease in concentration of Au ions (5.5 ppm, 4.52 ppm, 3.80 ppm, 3.12 ppm, 2.44 ppm, 1.14 ppm, 0.85 ppm and 0.04 ppm at 0 min., 2 min., 4 min., 5 min., 6 min., 7 min., 8 min. and 10 min respectively) indicating the conversion of Au ions into GNPs (Fig. 9).

TEM Analysis : A TEM image of the prepared gold nanoparticles is shown at 200 nm. The GNPs seen are roughly spherical in shape and morphology. The TEM images taken after 3 months shows the stability of biosynthesized GNPs.

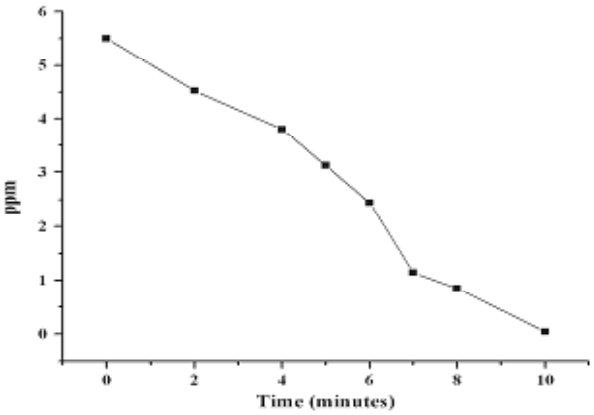

Fig. 9 : AAS graph of $HAuCl_4$ concentration.

DLS Analysis : DLS pattern reveals that gold nanoparticles synthesized by this method have a Zeta average diameter of 64.33± 3.56 nm with poly dispersity index (PDI) of 0.220. The DLS measured size is slightly bigger as compared to the particle size measured from TEM micrographs because dynamic light scattering method measures the hydrodynamic radius.

FTIR Analysis : FTIR measurements were carried out to identify the possible interaction between protein and gold nanoparticles (Fig. 5). Results of FTIR showed sharp absorption peaks at 1077 cm^{-1}, 1735 cm^{-1}, 2917 cm^{-1} and 3418 cm^{-1}.

Peak at 1077 cm^{-1} is assigned as the absorption peaks of –C–O–C– or –C–O–.Absorption peak at 1735 cm^{-1} corresponds to carbonyl stretch vibrations in ketones, aldehydes and carboxylic acids. Band at 2917 cm^{-1} is assigned to C–H stretching region. Peak at 3418 cm^{-1} is characteristic of –NH stretching of amide (II) band.

Apart from this the spectrum also shows peaks at 715 cm^{-1} and 837 cm^{-1}. Peak at 715 cm^{-1} is due to C–S stretching modes of the sulfur-bearing residues which confirm the presence of cysteine and methionine.

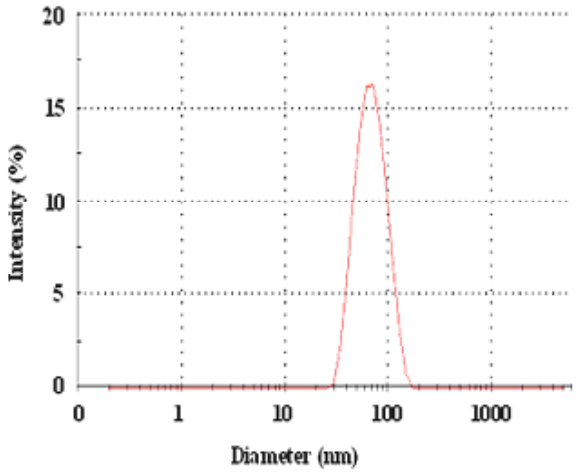

Fig. 10 : DLS pattern of biosynthesized gold nanoparticles. Diameter of the nanoparticles is found to be approximately in range of 5 nm to 40 nm with mean diameter of 16.046±3.2 nm. It was also observed that GNPs are evenly distributed in the sample.

C–H bend at 837 cm^{-1} could be well assigned to the aromatic residue tyrosine. These IR spectroscopic studies confirmed that carbonyl group of amino acid residues have strong binding ability with metal which suggests that they form a layer covering metal nanoparticles and acting as capping agent to prevent agglomeration and providing stability to the medium. It is known that with the help of free amino groups or cysteine groups, proteins can bind to gold nanoparticles. Thus, possibly here also gold nanoparticles are stabilized by surface-bound proteins. These results confirm the presence of possible proteins acting as reducing and stabilizing agents for gold nanoparticles.

XRD Analysis : The XRD analysis showed diffraction peaks corresponding to fcc structure of gold. Diffraction peaks observed at 2θ; 38.2º, 44.4º, 64.6º and 77.5º couldbe indexed to the (111), (200), (220) and (311) planes of a pure face centred crystalline structure of Au (JCPDS: 04-0784). The broadening of the Bragg peaks indicates the formation of nanoparticles. Full width at half maximum (FWHM) data was used with Scherrer's formula to determine the average particle size. The average particle size estimated was approximately 17 nm.

4. SUMMARY AND CONCLUSION

GNP synthesized from *Benincasa hispida :*

Biosynthesis of stable and spherical gold NPs using the extract of B. hispida seeds is simple, economic, nontoxic and efficient. The quantity of extract, reaction temperature and pH are found to play a critical role in the size dispersity of NPs. The nanoparticles are more stable at pH 6. Crystalline nature of NPs is evident from bright circular spots in the SAED pattern, clear lattice fringes in the HRTEM images and peaks in the XRD pattern. From FTIR spectrum, it is found that the possible reducing agent is polyols and the capping material responsible for stabilization is proteins present in the extract. The as-prepared GNPs showed good optical limiting behavior. The present investigation will lead to the development of a rational biosynthetic procedure for other metal NPs such as silver, platinum and palladium using the extract of *B. hispida* seeds.

GNP synthesized from *Justicia gendarussa :*

The reduction of gold ions by *Justicia gendarussa* leaves extract has been reported here. The diethyl ether phytochemical fraction have more polyphenol and flavonoid contents which produce maximum GNPs within 15 minutes compared to the chloroform and ethyl acetate phytochemical fractions of *Justicia gendarussa* leaves. The diethyl ether phytochemical fraction reduced gold nanoparticles shows maximum absorbance wavelength at 536 nm with different morphologies such as spherical, triangle, truncated triangle and hexagonal shapes. Theaverage size of diethyl ether phytochemical fraction reduced GNPs is 27 nm and stable for reasonable period of 5 months and at pH above the 7. The functional groups such as alcohols, phenols, aromatic amines, aliphatic amines, carboxyl groups present in Et_2O-PF are involved in reduction and capping of GNPs. This method proved that

nontoxic plant material has tremendous benefits and is eco-friendly and compatible for biomedical applications. Biosynthesis of GNPs by *Justicia gendarussa* leaf is simple, rapid, nontoxic and scalable for large scale synthesis.

GNP synthesized from *Ocimum basilicum :*

The present research work shows that leaf extract of *Ocimum basilicum* can be used efficiently for eco friendly bioreduction of $HAuCl_4$ into gold nanoparticles of average diameter of 16.046±3.2 nm within 10 minutes of reaction time. These nanoparticles were crystalline in nature and were stable upto 3 months. The synthesized gold nanoparticles are stable due to the presence of proteins acting as capping and reducing agents. Still, the biochemical pathway and mechanism of nanoparticles synthesis using leaf extract is not yet fully understood and needs to be explored. Some researches suggest the possible role of oxidoreductase enzymes which shuttles electrons in the reduction process.(A. Ahmad et al) Such theory was supported by the work done on bioconversion of silver and gold nanoparticles using fungus *Fusarium oxysporium* (P. Mukherjee et al.) and *Trichoderma viridae*.(A. M. Fayaz et al) Some researchers supported that the polyol components and the water soluble heterocyclic components such as alkaloid and flavones were principally responsible for the reduction of gold ions and the stabilization of the nanoparticles.(J. K. Andeani et al.) It is also known that *Ocimum* sp. Contains ascorbic acid which may be also responsible for reduction process.(I. Sondi et al.)

ACKNOWLEDGMENTS

GNP synthesized from *Benincasa hispida* :

The authors are pleased to acknowledge NIIST, Thiruvanantha- puram, for TEM measurements and Raman Research Institute (RRI), Bangalore, for providing the facility for nonlinear optical measurements.

GNP synthesized from *Justicia gendarussa* :

The authors gratefully acknowledge Dr. PushpaViswanathan, Professor, Cancer Institute (WIA), Chennai, India, for her immense support in analyzing samples under Tranmission Electron Microscope.

GNP synthesized from *Ocimum basilicum* :

We heartly acknowledge Dr. A.K.Chauhan for his support and for providing facilities for the fulfillment of this research work. We also acknowledge Dr. Richa Krishna for her guidance.

REFERENCES

Ahmad, A., Mukherjee, P., Senapati, S., Mandal, D., Khan, M. I. and Kumar, R., *Coll. Surf. B Biointerfaces* 28, 313 (2003).

Andeani, J. K., Kazemi, H., Safavi, A., and Mohsenzadeh, S., *Dig. J. Nanomat. Biostruc.* 6, 1011 (2011).

Ankamwar, B., Chaudhary,M. and Murali, S., Synth. React. Inorg. Met.-org. Nanometal. Chem., 35, 19 (2005).

Aswathy Aromal, S., Daizy Philip, Physica, doi:10.1016/ j.physe.02.013 (2012).

Badri Narayanan, K. and Sakthivel, N., Mater. Charact., 61, 1232 (2010).

Borchert, H., Shevchenko, E.V., Robert, A., Mekis, I., Kornowski, A., Grubel, G., Langmuir 21, 931 (2005).

Chin Wee Shong, Sow Chorng Haur, Andrew T., and Wee, S. , Science at the nanoscale: An introductory textbook: Pan Stanford Publishing.heim, pp 7-22 (2010).

Chuang, Y.C., Li, J.C., Chen, S.H., Liu, T.Y., Kuo, C.H., Huang , W.T. and Lin, C.S., Biomater., 31, 6087 (2010).

Cumberland, S.L., Strouse, G.F., Langmuir 18, 269(2002).

Das, P.K., Borthakurb, B.B. and Bora, U., Mater. Lett. 64, 1445 (2010).

Fayaz, A. M., Balaji, K., Girilal, M., Yadav, R., Kalaichelvan, P. T. and Venketesan, R., *Nanomed. Nanotechnol. Biol. Med*. 6, 103 (2010).

Garima Singhal, Riju Bhavesh, Ashish Ranjan Sharma, and Rajendra Pal Singh; Advanced Science, Engineering and Medicine Vol. 4, pp. 62–66, (2012).

Gole, A., Dash, C., Ramachandran, V., Rao, M., Mandale, A. B., Sainkar, S. R. and Sastry, M., *Langmuir* 17, 1674 (2001).

Guo, Z., Fan, X., Liu, L., Bian, Z., Gu, C., Zhang Y., Gu, N., Yang, D. and Zhang, J., J. Colloid. Int. Sci., 348, 29 (2010).

Huang, N. M., Lim, H. N., Radiman, S., Khiew, P. S., Chiu, W. S., Hashin, R. and Chia, C. H., *Colloids Surf*. 353, 69 (2010).Khlebtsov, N.G. and Dykman, L.A.. Quan, J.. Spect. Radiative Transfer, 111, 1 (2010).

Klug, H. P. and Alexander, L. E., X-Ray Diffraction Procedures for Polycrystalline and Amorphous Materials, Wiley, New York (1974).

Li, S., Shen, Y., Xie, A., Yu, X., Zhang, X., Yang, L. and Li, C., Nanotechnology 18, 405101 (2007).

Manickam Chinna, Ponnuswamy Renuka Devi, Asthanari Saravanakumar , Venseslas Femi, Eswaran Hemananthan and Soundharajan Senthil Rani; Chinna *et al.*, IJPSR; Vol. 3(2): 623-629 (2012).

Mukherjee, P., Ahmad, A., Mandal, D. S., Senapati, S., Sainkar, R., Khan, M. I., Parishcha, R., Kumar, R., Ajaykumar, P. V., Alam, M. and Sastry, M., *Nano Lett*. 1, 515 (2001).

Mulvaney , P., *Langmuir* 12, 788 (1996).

Narayanan K. B. and Sakthivel N., *Mater. Lett*. 62, 4588 (2008).

Philip D., Spectrochimica Acta Part A 73, 374(2009).

Philip, D. and Unni, C., *Physica E*. 43, 1318 (2010).

Philip, D., Physica E 42, 1417 (2010).

Qudrie, Z.L., Anandan, Ashraf, H., R., Mushtaque, Md., and Kumar, K.A.,Pharmaco- logyonline 2, 1298 (2011).

Reddi, G. S., and. Rao, C.R.M, *Trends in analytical chemistry,* vol. 19, no. 9 (2000).

Sanghi ,R., and Verma P., *Adv. Mater. Lett*. 1, 193 (2010).

Sathyavathi, R., Krishna, M. B., Rao, S. V., Saritha, R., and Rao, D. N., *Adv. Sci. Lett*. 3, 1 (2010).

Sheny, D.S, Mathew, J., Philip, D., Spectrochimica Acta Part A 79, 254 (2011).

Smitha, S.L., Philip, D., Gopchandran, K.G., Spectrochimica Acta Part A 74 735 (2009).

Sondi, I., Goia, D. V. and Matijevi'c E., *J. Coll. Interface Sci*. 260, 75 (2003).

Sulabha K. Kulkarni, Nanotechnology: Principles & practices: Capital Publishing Company (2009).

Toderas, F., Iosin M., Astilean, S., Nuclear Instruments and Methods in Physics Research B 267 400(2009).

Wang, H., Zheng, L., Peng, C., Guo, R., Shen, M., Zhang, G. and Shi, X., Biomate., 32, 2979 (2011).

Zhu, M., Apparatus Analyses, Higher Education, Beijing (2000).